SPURIOUS PASS-BAND SUPPRESSION IN COUPLED-SERIAL-SHUNTED LINES WIDEBAND BAND-PASS FILTERS

L.-C. Tsai[*]

Department of Electronic Engineering, Lunghwa University of Science and Technology, 300 Wanshou Rd., Sec. 1, Guishan Shiang, Taoyuan 33306, Taiwan, R.O.C.

Abstract—In this paper, a synthesis method is presented for Chebyshev type II band-pass filters in the microwave frequency range. We investigate the cause of the second harmonic passband of coupled-serial-shunted lines bandpass filters. Filters are employed substrate suspension, wavy-edge coupling, ring resonators, defect ground structure (DGS), and a combination of the wavy-edge coupling and ring resonators may be used and were investigated to suppress the harmonic pass-band. With a combination of the wavy-edge coupled-lines and ring resonators, the harmonic pass-band of the parallel-coupled line filter is rejected more effectively. Several filters are fabricated and measured to demonstrate the design.

1. INTRODUCTION

Parallel-coupled lines make up the structure of a band-pass filter, which has been widely used in various communication systems [1–6] to reduce production costs and improve usefulness effectively. However, its shortcoming is the second harmonic, which leads to the trend of increasingly serious noise interference between bands faced by the communications industry [1, 5]. Undesired harmonics is a limitation of microwave circuits, which can seriously degrade their performance and critical in applications. The noises at both sides of the band-pass are easy to make filter attenuation insufficient, which impacts the system performance. An additional band-pass filter is cascaded to improve the overall out-of-band; however, they increase the device area

and introduce additional insertion losses. The second parasitic pass-band of a parallel coupled-line filter only exists for transmission line structures of quasi-TEM, such as microstrip or coplanar waveguide. that the phase velocity of the even and odd mode propagation is not the same.

To overcome this difficulty, many researchers have investigated this problem [7–21]. Kuo and Lin [7] use stepped-impedance resonators with different dimensions extended upper stop-band. Lopetegi et al. [8] employ a continuous perturbation of the width of the coupled-lines following a sinusoidal law to achieve multi-spurious rejection. Electromagnetic band-gap (EBG) and defected ground structure have been introduced as a means to achieve harmonic suppression in microwave circuits [9]. Employing square periodic grooves improve the harmonic suppression characteristics at the twice pass-band frequency [10]. To achieve suppression of second harmonic, we employ the substrate suspension, to improve the harmonic pass-band in coupled-serial-shunted lines Chebyshev type II band-pass filters.

The motivation of this work is to explore a nonconventional method to design wideband bandpass filters in coupled-serial-shunted lines by using the discrete-time domain technique. To design a band-pass filter, we first choose an ideal discrete-time filter. Based on zero locations of the ideal digital filter, we configure the transmission-line network consisting of parallel-coupled lines (PCLs), two-section open circuited stubs, and serial transmission line to form a new structure so that the transfer function of transmission-line can emulate the ideal digital filter. Each PCL contributes a zero at $z = 1$ that provides a steeper descent near the stop-band. The two-section open-circuited shunt stub, however, contributes a pair of conjugate zeros located on the unit circle in the z-plane. Chebyshev type II band-pass filters are implemented in microstrip formats. The close agreement between theoretical values and experimental results illustrates the validity of this method. This paper is organized as follows. Section 2 briefly describes and discusses five methods for second-harmonic suppression. Section 3 presents the design procedures of chebyshev type II band-pass filters. The experimental and simulated results are also presented in Section 3. Finally, Section 4 briefly draws some conclusions.

2. METHODOLOGY

2.1. Wavy-edge Coupling

As shown in Figs. 1(a)–(b), the odd-mode phase velocity is faster than the even-mode, and the even-mode and odd-mode per unit length

capacitances are expressed as follows:

$$C_e = C_f + C_p + C_{fe} \tag{1a}$$

$$C_o = C_f + C_p + C_{fo} \tag{1b}$$

where C_p is the parallel-plate capacitance and C_f the fringing capacitance. C_{fe} and C_{fo} are the stray capacitances of even- and odd-mode lines, respectively.

By increasing odd-mode transmission distance, the phase velocities of odd and even modes can be equal. As shown in Fig. 1(c), C_{ow} is the odd-mode per unit length capacitance. The effective dielectric constants of odd and even modes are the same and equal to the even mode in wavy-edge coupling microstrip line. Therefore, the odd-mode capacitance per unit length C_{ow} of wavy-edge coupling microstrip line can also be expressed

$$C_{fow} = C_{ow} + C_{fo}. \tag{2}$$

Fig. 2 shows the wavy-edge coupling microstrip lines and physical dimensions. The capacitance distribution and unit length of wavy-edge coupling microstrip line is

$$C_{ow} = X_w. \tag{3}$$

The relationship between unit length Δx and wavy-edge depth d_t is

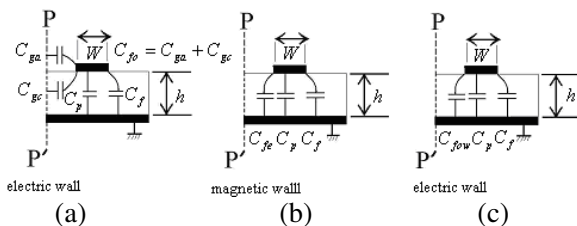$$X_w = 2d_t + \Delta x. \tag{4}$$

Figure 1. Wavy-edge coupling microstrip line. (a) Odd mode. (b) Capacitance distribution model in even-mode static transmission line. (c) Odd-mode capacitance per unit length C_{ow} of modified wavy-edge coupling microstrip line.
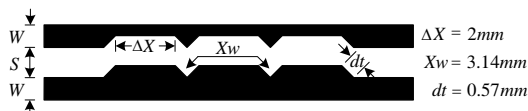

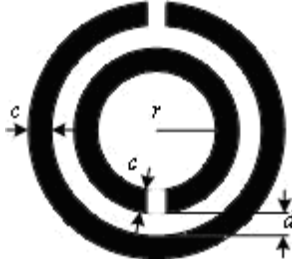**Figure 2.** The wavy-edge coupling microstrip lines and physical dimensions.

Figure 3. The input and output ports of the split rings physical dimensions. $r = 1.8\,\text{mm}$ and $c = d = 0.2\,\text{mm}$.

where the physical dimensions of wavy-edge coupling sections are $\Delta x = 2\,\text{mm}$, $X_w = 3.14\,\text{mm}$, and $d_t = 0.57\,\text{mm}$.

2.2. Ring Resonators

Ring resonators [11, 12] can be equivalent to a parallel resonant circuit of the capacitor and inductor. With the resonant frequency, the input signal with the ring structure cannot completely reach the output port. Enhancing the coupling between feed side and ring resonators is to couple the ring resonators with taps between input and output ports.

The resonant frequency is [22]

$$f_0 = \frac{1}{2\pi\sqrt{LC}},\tag{5}$$

where L and C are parallel connection of the inductor and capacitor resonator. The parallel circuit of the inductor and capacitor is equivalent to a band-stop filter [14]; however, to achieve an effective rejection band, fine tuning has to be implemented. Three split ring pairs have been etched around input and output ports to attenuate the first harmonic bands. The detailed dimensions of the structures are shown in Fig. 3. The ring resonators and feed lines are directly connected. From Eq. (5), the specific frequency is obtained to achieve the second harmonic suppression.

2.3. DGS

Figure 4(a) shows the bottom side of the filter physical dimensions with two DGSs at input and output ports. The DGS equivalent circuit is based on a parallel resonant circuit. If the circuit is lossless, it is a L-C parallel resonant circuit. The equivalent L-C parallel circuit of the DGS can be obtained because this type of electrical characteristic is
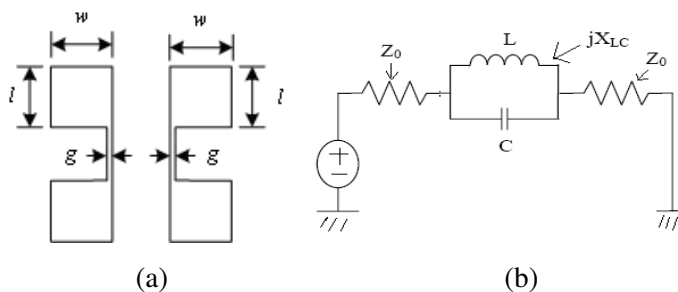
Figure 4. (a) The bottom side of the filter physical dimensions with DGS. $w = 3.5\,\mathrm{mm}$, $l = 3.45\,\mathrm{mm}$, and $g = 0.3\,\mathrm{mm}$. (b) The equivalent circuit of the DGS resonator.

observed from a typical L-C parallel resonant circuit. The suppression effect can be achieved in a specific frequency [15].

The basic equivalent circuit of the DGS resonator is shown in Fig. 4(b). The parameters of the equivalent circuit can be used to suppress band-pass frequency response. The two reactance values of the equivalent L-C parallel resonant circuit are [15]

$$X_{LC} = \frac{1}{\omega_0 C \left(\frac{\omega_0}{\omega} - \frac{\omega}{\omega_0} \right)}, \tag{6}$$

where ω_0 is the L-C resonant angular frequency and C the equivalent capacitance. In the case with $\omega = \omega_c$, the equivalent capacitance C can be obtained as follows:

$$C = \frac{1}{2Z_0 \omega_0 \left(\frac{\omega_0}{\omega} - \frac{\omega}{\omega_0} \right)} = \frac{\omega_c}{2Z_0 \left(\omega_0^2 - \omega_c^2 \right)}, \tag{7}$$

where Z_0 is the characteristic impedance of DGS transmission line and ω_c the band-pass filter resonant angular frequency.

2.4. Substrate Suspension

The intuitive method for parallel coupled-lines filters with suppression of spurious responses using a substrate suspension can be as follows. The structure adds a second medium layer on the original foundation plate [20, 21]. For the substrate suspension structure shown in Fig. 5, to eliminate second harmonic, substrate suspension makes the microstrip phase velocities of odd and even-modes equal. The structure of aerosol foundation plate can significantly inhibit the second harmonic response.
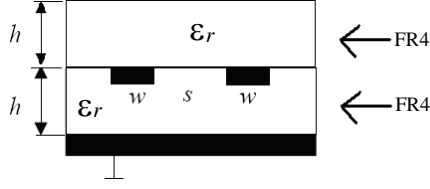
Figure 5. The configuration of substrate suspension.

3. EXPERIMENTAL RESULTS

Table 1 shows chain-scattering parameter matrices T_{ij} (i, $j = 1$, 2) of a serial line, a two-section open-circuited shunt stub, and a PCL in the Z domain. A serial line contributes to one zero at $z = 0$; a two-section open-circuited shunt stub contributes to two zeros locating on the unit circle; a PCL contributes to one zeros at $z = 1$. If the configuration consists of K two-section open-circuited shunt stubs, L serial lines, and M PCLs, then the matrix element $T_{11,\,\text{overall}}(z)$ of the overall network is expressed as follows:

$$T_{11,\,\text{overall}}(z) =$$
$$\frac{\displaystyle\sum_{i=0}^{2K+L+2M} d_i z^{-i}}{\displaystyle\prod_{k=1}^{K}(1+2\gamma_k z^{-1}+z^{-2})\prod_{l=1}^{L}z^{-L/2}(1-\Gamma_l^2)\prod_{m=1}^{M}z^{-M/2}(1-z^{-1})}. \quad (8)$$

According to Eq. (8), all d_i are real and determined by the characteristic impedance of all transmission-line components. When the output of the cascade network is properly terminated, we obtain the transfer function $T(z)$ of such a transmission-line network as follows:

$$T(z) = \frac{1}{T_{11,\,\text{overall}}(z)} = z^{-(M+L)/2}\frac{\displaystyle\prod_{k=1}^{K}(1+2\gamma_k z^{-1}+z^{-2})\prod_{m=1}^{M}(1-z^{-1})}{\displaystyle\sum_{i=0}^{2K+L+2M} A_i z^{-i}}, \quad (9)$$
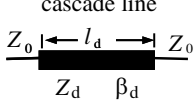
where $A_i = d_i/(\prod_{l=1}^{L}(1-\Gamma_l^2))$ is a function of the characteristic impedances of all PCL, two-section open circuited shunt stubs, and serial transmission-line elements. To implement the filters with transmission lines, the electrical length of each transmission-line section is set equal to $90°$ at the normalizing frequency. We have $l = \lambda_0/4$, where l represents the physical length of each transmission line section and λ_0 the wavelength at the normalizing frequency.

As an example, we assume that the central frequency of the filter is 3.5 GHz with 46 dB ripple in the stop-band. A discrete-time Chebyshev type II band-pass filter prototype is [21]

$$F(z) = \frac{\sum_{j=0}^{5} b_j z^{-j}}{\sum_{i=0}^{5} a_i z^{-i}}, \tag{10}$$

where $\{b_j, 0 \le j \le 5\} = \{0.0190, -0.0169, 0.0317, -0.0317, 0.0169, -0.0190\}$, and $\{a_i, 0 \le i \le 5\} = \{1.0000, 2.4063, 2.7139, 1.6204, 0.5152, 0.673\}$. To construct band-pass filters, we employ microstrip lines to emulate transmission lines. The microstrip lines are assumed to be

Table 1. Basic transmission line elements chain-scattering parameter matrices.

$$\begin{bmatrix} T_{11} & T_{12} \\ T_{21} & T_{22} \end{bmatrix}$$

cascade line

$$\frac{1}{z^{-1/2}(1-\Gamma^2)} \begin{bmatrix} 1-\Gamma^2 z^{-1} & -(\Gamma-\Gamma z^{-1}) \\ \Gamma - \Gamma z^{-1} & -\Gamma^2 + z^{-1} \end{bmatrix} \quad \text{where } \Gamma = \frac{Z_d - Z_0}{Z_d - Z_0}$$

two-section shunt-open
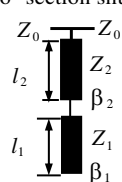
$$\frac{1}{D(z)} \begin{bmatrix} \dfrac{2Z_2 D(z) + Z_0 C(z)}{2Z_2} & \dfrac{Z_0 C(z)}{2Z_2} \\ -\dfrac{Z_0 C(z)}{2Z_2} & \dfrac{2Z_2 D(z) - Z_0 C(z)}{2Z_2} \end{bmatrix}$$

where $C(z) = 1 - z^{-2}$,

$D(z) = 1 + 2\gamma z^{-1} + z^{-2}$

$\gamma = \dfrac{Z_1 - Z_2}{Z_1 + Z_2}$

parallel-coupled line

$$\frac{1}{8c_2 Z_0 z^{-1/2}(1-z^{-1})} \begin{bmatrix} l_1 & -n_1 \\ n_1 & p_1 \end{bmatrix}$$

where

$l_1 = (4c_1 Z_0 + c_1^2 + 4Z_0^2) + (2c_1^2 - 4c_2^2 - 8Z_0^2)z^{-1}$
$\quad + (-4c_1 Z_0 + c_1^2 + 4Z_0^2)z^{-2}$
$n_1 = (c_1^2 - 4Z_0^2) + (2c_1^2 - 4c_2^2 + 8Z_0^2)z^{-1}$
$\quad + (c_1^2 - 4Z_0^2)z^{-2}$
$p_1 = (4c_1 Z_0 - c_1^2 - 4Z_0^2) + (2c_1^2 + 4c_2^2 + 8Z_0^2)z^{-1}$
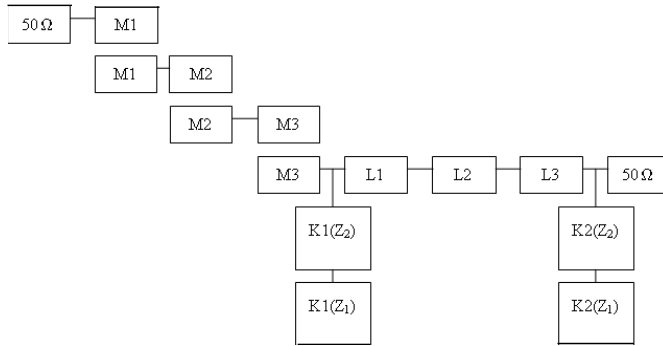$\quad + (-4c_1 Z_0 - c_1^2 - 4Z_0^2)z^{-2}$

Figure 6. The configuration of a Chebyshev type II band-pass filter.

both lossless and dispersionless for the present consideration. Because of the limitation caused by the available manufacturing technique, the line width of the serial line and shunt stub is limited to 0.1 mm. In addition, the small gap size of PCL is limited to 0.1 mm. Therefore, the largest value of all characteristic impedances is limited to 160 ohms, and the large range of the characteristic impedances of even- and odd-mode is limited. There exist five zeros in $F(z)$ which are $z = 1, -0.2630 \pm 0.9648i$, and $0.2088 \pm 0.9780i$. Under such a condition, we may select one PCL, two two-section open-circuited stubs, as well as series line as the basic network. The next step is to compare the coefficients of denominators in (9) so that $T(z)$ is as close to $F(z)$ as possible. Notice that A_i in (9) is determined by the characteristic impedance of all transmission lines. Upon using the optimization method in the sense of minimum square error for the coefficients of denominators on (9) and (10), the optimization algorithm [23, 24] gives $K = 2$, $L = 3$, and $M = 3$. Fig. 6 shows the pattern of the network used to synthesize the band-pass filter in (10). The even- and odd-mode characteristic impedances of PCLs in Fig. 6 are ($M_1 = 159.4$ and 49.7, $M_2 = 113$ and 47.4, $M_3 = 120.8$ and 69.3) ohms. The characteristic impedances of the serial lines are ($L_1 = 36.5$, $L_2 = 76.7$, $L_3 = 63.3$) ohms. In addition, the characteristic impedances of two two-section open-circuited stubs are ($K_1(Z_2) = 26$, $K_1(Z_1) = 44.6$, $K_2(Z_2) = 160$, $K_2(Z_1) = 104.7$) ohms.

We measured the reflected and transmitted parameters by using an Agilent N5230A network analyzer. Fig. 7 shows the measured original $|S_{21}|$, wavy-edge $|S_{21}|$, $|S_{11}|$, and ideal of the Chebyshev type II band-pass filters. In Fig. 7, the second harmonic band of the original filter measured $|S_{21}|$ is about -13 dB. After using wavy-edge coupling, the filter measured $|S_{21}|$ is suppressed to -25 dB ([10] has measured

-20 dB with groove number of 3). The slight difference between
the theoretical values $|S_{21}|$ and measured results $|S_{21}|$ in the lower
frequency band is due to conductor loss, dielectric loss, as well as the
limitation of manufacturing. Fig. 8 shows the measured $|S_{21}|$ and $|S_{11}|$
of the ring resonators. As shown in Fig. 8, the second harmonic of
measured $|S_{21}|$ is suppressed by the ring resonators to about -30 dB
([11] is about -30 dB). All prototypes filters have been fabricated
on the same substrate as mentioned previously. The photograph of
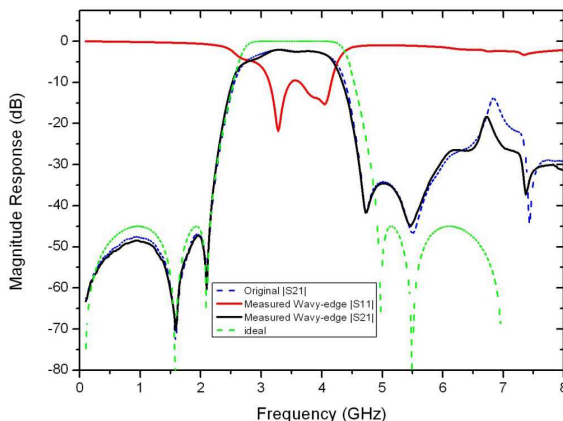the DGS is shown in Fig. 9. Fig. 10 shows the measured $|S_{21}|$ and

Figure 7. Measured $|S_{21}|$ and $|S_{11}|$ for Chebyshev type II band-pass
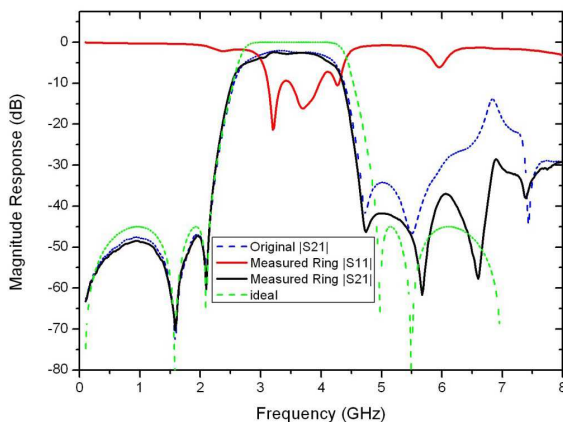filter with the wavy-edge coupling.

Figure 8. Measured $|S_{21}|$ and $|S_{11}|$ for Chebyshev type II band-pass
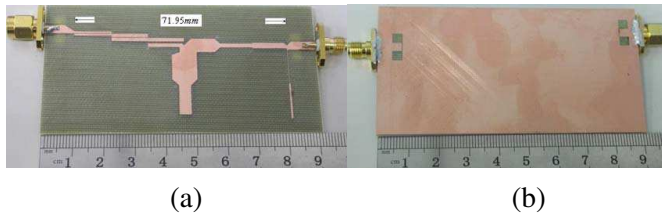filter with the ring resonators.

(a)   (b)

Figure 9. Fabricated Chebyshev type II band-pass filter with DGS. (a) Top view. (b) Bottom view.
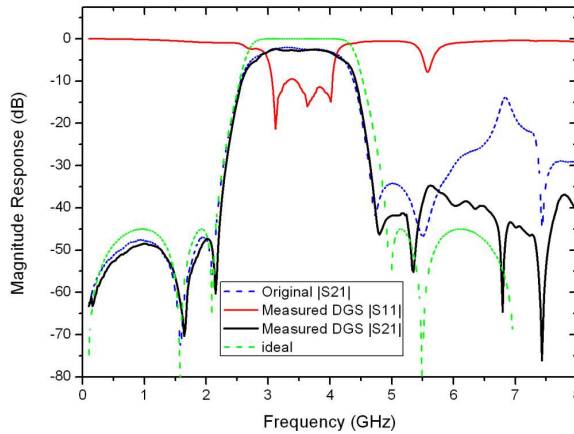

Figure 10. Measured $|S_{21}|$ and $|S_{11}|$ for Chebyshev type II band-pass filter with the DGS.

$|S_{11}|$ using the DGS. In Fig. 10, the second harmonic of the DGS is suppressed to about -40 dB ([15] is about rejection of 40 dB). The filter is built on a FR4 substrate having a thickness of 1.6 mm, relative dielectric constant of 4.4, and loss tangent $\tan\delta =0.018$. The left-hand side of the network is port 1, and the right-hand side is port 2. On both sides, the reference impedance lines ($50\,\Omega$) are placed, and all finite transmission lines have electrical length of $90°$ at 3.5 GHz. The total length of the filter excluding reference lines on both sides is 71.95 mm. In particular, the big difference in characteristic impedances will cause a large discontinuity effect. By using mitering, the discontinuity effect can be largely reduced. The mitering method is employed for $K_1(Z_2)$ and L_1 the discontinuity effect. However, we compared the measured $|S_{21}|$ with the ideal $|S_{21}|$; because of the effect of discontinuities of steps, T-junctions, and open-circuited ends of the components, the pass-band bandwidth of measured $|S_{21}|$ (1.5 GHz) is smaller than that of the ideal $|S_{21}|$ (1.7 GHz).

Figure 11 shows the photograph of the combination of the wavy-edge coupling and ring resonators. The physical dimensions of Chebyshev type II band-pass filter is shown in Fig. 11. The total length of the filter including reference lines on both sides is 108.65 mm. Fig. 12 shows measured $|S_{21}|$ of Fig. 11 which is suppressed to about -50 dB; at least -35 dB of the first spurious band is obtained. In addition, other combinations cannot obtain a good suppression because the top side of the planar circuit and the bottom side of the DGS will interact. Fig. 13 shows the photograph of aerosol foundation plate. Fig. 14
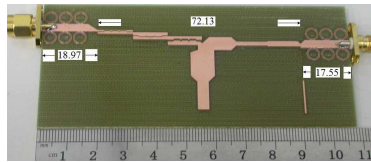

Figure 11. Fabricated Chebyshev type II band-pass filter with combination of the wavy-edge coupling and the ring resonators.
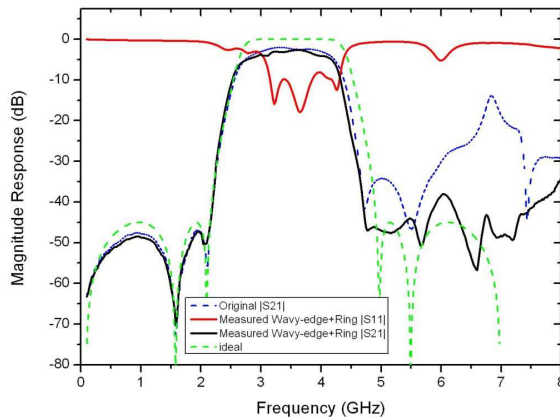

Figure 12. Measured $|S_{21}|$ and $|S_{11}|$ for Chebyshev type II band-pass filter with combination of the wavy-edge coupling and the ring resonators.

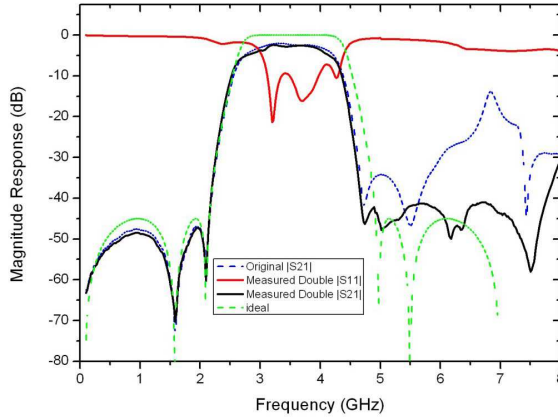**Figure 13.** The photograph of the aerosol foundation plate.

Figure 14. Measured $|S_{21}|$ and $|S_{11}|$ for Chebyshev type II band-pass filter with substrate suspension.

Table 2. The comparison of the harmonic band suppresses methods.

The harmonic band suppress methods	Magnitude of second harmonic band	References
Wavy-edge coupling	$-25\,\mathrm{dB}$	$-20\,\mathrm{dB}$ [10]
Ring resonators	$-30\,\mathrm{dB}$	$-30\,\mathrm{dB}$ [11]
Defected ground structures	$-40\,\mathrm{dB}$	$-40\,\mathrm{dB}$ [15]
Combination of wavy-edge coupling and ring resonators	$-50\,\mathrm{dB}$	none

shows the measured $|S_{21}|$ and $|S_{11}|$ of the substrate suspension. In Fig. 14, the second harmonic suppression of the substrate suspension measured $|S_{21}|$ is about $-45\,\mathrm{dB}$. Due to loss factors of the substrate, conductor, and two SMA connectors, the magnitude of measured S_{21} over the passband is approximately $-2.5\,\mathrm{dB}$ compared to the ideal value $0\,\mathrm{dB}$. The measured response sinks in the upper stop-band for the combination of the wavy-edge coupling and ring resonators, which is below $-55\,\mathrm{dB}$ and the substrate suspension also below $-55\,\mathrm{dB}$. Employing the same synthesis method shown in [23, 24] and the same substrate as mentioned previously, we obtain the Chebyshev type II band-pass filters with four second harmonic suppression methods listed in Table 2. Substrate suspension has second-harmonic suppression of 40–45 dB. Combination of the wavy-edge coupling and ring resonators has the best second harmonic suppression of 45–50 dB.

4. CONCLUSION

In this study, an equal-length microstrip network was implemented to emulate the characteristics of Chebyshev type II band-pass filters. Five methods for second-harmonic suppression are presented. The comparison between filter characteristics, according to the substrate suspension, wavy-edge coupling, ring resonators, and DGS, has been studied. Five circuits are fabricated and measured to demonstrate the formulation and circuit synthesis. In ring resonators case, the split rings have been etched at both sides of the $50\,\Omega$ lines and designed to suppress the first spurious band. Moreover, the wavy-edge coupling technique provides more design flexibility to reject spurious passbands in parallel-coupled line. In particular, a combination of the wavy-edge coupling and ring resonators is employed to suppress first spurious pass-band. The measured results of the wavy-edge coupling and ring resonators show harmonic rejection levels more than $35\,dB$. As a result, the advantages of low cost and easy fabrication have been obtained.

ACKNOWLEDGMENT

REFERENCES

1. Pozar, D. M., *Microwave Engineering*, 2nd edition, Ch. 8, Wiley, New York, 1998.
2. Cohn, S. B., "Parallel-coupled transmission-line-resonator filters," *IEEE Trans. Microw. Theory Tech.*, Vol. 6, No. 4, 223–231, Apr. 1958.
3. Cristal, E. G. and S. Frankel, "Hairpin-line and hybrid hairpin-line/halfwave parallel-coupled-line filters," *IEEE Trans. Microw. Theory Tech.*, Vol. 20, No. 11, 719–728, Nov. 1972.
4. Hong, J. S. and M. J. Lancaster, "Design of highly selective microstrip bandpass filters with a single pair of attenuation poles at finite frequencies," *IEEE Trans. Microw. Theory Tech.*, Vol. 48, No. 7, 1098–1107, Jul. 2000.
5. Hong, J.-S. G. and M. J. Lancaster, *Microstrip Filter for RF/Microwave Application*, Wiley, New York, 2001.
6. Lee, S. Y. and C. M. Tsai, "New cross-coupled filter design using improved hairpin resonators," *IEEE Trans. Microw. Theory Tech.*, Vol. 48, No. 12, 2482–2490, Dec. 2000.

7. Kuo, J. T. and H. P. Lin, "Dual-band bandpass filter with improved performance in extended upper rejection band," *IEEE Trans. Microw. Theory Tech.*, Vol. 57, No. 4, 824–828, Apr. 2009.

8. Lopetegi, T., M. A. G. Laso, F. Falcone, F. Martin, J. Bonache, J. Garcia, L. Perez-Cuevas, M. Sorolla, and M. Guglielmi, "Microstrip 'wiggly-line' bandpass filters with multispurious rejection," *IEEE Microw. Wireless Compon. Lett.*, Vol. 14, No. 11, 531–533, Nov. 2004.

9. Lopetegi, T., M. A. G. Laso, M. J. Erro, D. Benito, M. J. Garde, F. Falcone, and M. Sorolla, "Novel photonic bandgap microstrip structures using network topology," *Microwave Opt. Technol. Lett.*, Vol. 25, 33–36, Apr. 2000.

10. Kim, B. S., J. W. Lee, and M. S. Song, "An implementation of harmonic-suppression microstrip filters with periodic grooves," *IEEE Microw. Wireless Compon. Lett.*, Vol. 14, No. 9, 413–415, Sept. 2004.

11. Joan, G.-G., F. Martin, F. Falcone, "Spurious passband suppression in microstrip coupled line band pass filters by means of split ring resonators," *IEEE Microw. Wireless Compon. Lett.*, Vol. 14, No. 9, 416–418, Sept. 2004.

12. Marques, R., F. Mesa, J. Martel, and F. Medina, "Comparative analysis of edge- and broadside-coupled split ring resonators of metamaterial design-theory and experiments," *IEEE Trans. Antennas Propagat.*, Vol. 51, No. 10, 2572–2581, Oct. 2003.

13. Chen, C.-F., T.-Y. Huang, and R.-B. Wu, "Design of microstrip bandpass filters with multi-order spurious-mode suppression," *IEEE Trans. Microw. Theory Tech.*, Vol. 53, No. 12, 3788–3793, Dec. 2005.

14. Mokhtaari, M., K. Rambabu, J. Bornemann, and S. Amari, "Advanced stepped-impedance dual-band filters with wide second stopbands," *Proc. Asia–Pacific Microw. Conf.*, 2285–2288, 2007.

15. Park, J. S., J. S. Yun, and D. Ahn, "A design of the novel coupled-line bandpass filter using defected ground structure with wide stopband performance," *IEEE Microw. Wireless Compon. Lett.*, Vol. 10, No. 9, 124–126, Sept. 2002.

16. Kuo, J.-T., W.-H. Hsu, and W.-T. Huang, "Parallel-coupled microstrip filters with suppression of harmonic response," *IEEE Microw. Wireless Compon. Lett.*, Vol. 12, No. 10, 383–385, Oct. 2002.

17. Hu, W. L., T. Yoshimasu, and H. W. Liu, "A novel dual-mode square loop passband filter with second spurious passband suppression," *International Conference Comm. Circuits and*

Systems Proceedings, Vol. 4, 2273–2276, Jun. 2006

18. Rehner, R., D. Schneiderbanger, M. Sterns, S. Martius, and L.-P. Schmidt, "Novel coupled microstrip wideband filters with spurious response suppression," *European Microwave Conference*, 858–861, Oct. 2007.

19. Ahn, D., J. S. Park, C. S. Kim, J. Kim, Y. Qian, and T. Itoh, "A design of low-pass filter using the novel microstrip defected ground structure," *IEEE Trans. Microw. Theory Tech.*, Vol. 49, 86–93, Jan. 2001.

20. Gupta, K. C., R. Gary, and I. J. Bahl, *Microstrip Lines and Slotlines*, Artech House, 1996.

21. Horno, M. and F. Medina, "Multilayer planar structures for high-directivity directional coupler design," *IEEE Trans. Microw. Theory Tech.*, Vol. 34, 1442–1449, Dec. 1986.

22. Pozar, D. M., *Microwave Engineering*, 2nd Edition, 160–163, Wiley, New York, 1998.

23. Oppenheim, A. V. and R. W. Schafer, *Discrete-Time Signal Processing*, Englewood Cliffs, Prentice-Hall, NJ, 1998.

24. Tsai, L.-C., K.-L. Chen, and C.-W. Hsue, "Design of wideband band pass filters using discrete time domain techniques," *Microwave and Optical Technology Letters*, Vol. 43, 264–266, Nov. 2004.